Acid-Induced Denaturation of Myoglobin Studied by Time-Resolved Electrospray Ionization Mass Spectrometry†

L. Konermann,‡ F. I. Rosell,§ A. G. Mauk,§ and D. J. Douglas*,‡

Department of Chemistry, University of British Columbia, Vancouver, British Columbia V6T 1Z1, Canada, and Department of Biochemistry and Molecular Biology, University of British Columbia, Vancouver, British Columbia V6T 1Z3, Canada

Received February 17, 1997; Revised Manuscript Received March 28, 1997⊗

ABSTRACT: The acid-induced denaturation of holo-myoglobin (hMb) following a pH-jump from 6.5 to 3.2 has been studied by electrospray ionization (ESI) mass spectrometry in combination with a continuous flow mixing technique (time-resolved ESI MS). Different protein conformations are detected by the different charge state distributions that they generate during ESI. The changes in intensity of the peaks in the mass spectrum as a function of time can be described by two exponential lifetimes of 0.38 ± 0.06 s and 6.1 ± 0.5 s, respectively. The acid-induced denaturation of hMb was also studied in stopped-flow experiments by monitoring changes in the Soret absorption. The lifetimes measured by this method are in good agreement with those obtained by time-resolved ESI MS. The shorter lifetime is associated with the formation of a transient intermediate which shows the mass of the intact heme−protein complex but leads to the formation of much higher charge states during ESI than native hMb at pH 6.5. This form of hMb has an absorption spectrum similar to that of the native protein, indicating a relatively unperturbed chromophore environment inside the heme binding pocket. The intermediate can thus be characterized as an unfolded form of hMb with essentially intact heme−protein interactions. The longer of the two lifetimes is associated with the formation of a product which has a blue-shifted absorption spectrum with a much lower maximum absorption coefficient than observed for native hMb. In the ESI mass spectrum, this product appears as the apoprotein with high charge states which indicates the disruption of the native heme−protein interactions and a considerable degree of unfolding compared to native apo-myoglobin. The mechanism of acid-induced denaturation of hMb, therefore, appears to follow the sequence $(\text{heme}-\text{protein})_{\text{native}} \rightarrow (\text{heme}-\text{protein})_{\text{unfolded}} \rightarrow \text{heme} + (\text{protein})_{\text{unfolded}}$.

The heme group in holo-myoglobin (hMb)[1] is noncovalently bound in a hydrophobic pocket and makes a large number of contacts with the protein (Takano, 1977; Evans & Brayer, 1990). These interactions include the coordination of the central iron with the proximal histidine (His^{93}) and hydrophobic interactions between the heme vinyl groups and apolar amino acid side chains. In addition, the heme propionate groups are oriented toward the surface of the protein where they are involved in electrostatic interactions with polar or charged amino acid residues (Takano, 1977; Evans & Brayer, 1990; Hargrove et al., 1996a,b; Hargrove & Olson, 1996). Unfolding of the protein induced by acidification of the solution is driven primarily by the protonation of histidine residues, including His^{93}, that are inaccessible to the solvent in the native conformation (Puett, 1973). This unfolding leads to the disruption of the iron−histidine bond and is accompanied by dramatic changes in the RR and absorption spectra of the heme group (Sage et al., 1991; Palaniappan & Bocian, 1994). The conformational changes of the protein and the disruption of the coordination bond lead to a weakening of the heme−protein interactions so that under these conditions the heme group can be easily extracted into an organic phase (Rossi-Fanelli et al., 1958; Teale, 1959). In the absence of an organic phase, the complete dissociation of the heme is hindered by its hydrophobicity so that in moderately acidic solutions (between pH 2.6 and pH 3.5) it remains associated with the protein (Sage et al., 1991). Under these conditions, hMb still retains about 50% of its native helical structure (Bismuto et al., 1983). It has been suggested that this form of the protein has structural features in common with the acid-induced molten globule of aMb (Hughson et al., 1990), although the binding of the heme may lead to formation of additional structure (Sage et al., 1991). Upon further decrease in pH, the protein eventually adopts a random coil structure (Griko et al., 1988; Palaniappan & Bocian, 1994).

In a recent study, time-resolved ESI MS has been applied to measure the refolding kinetics of acid-denatured cytochrome *c* (Konermann et al., 1997). This method uses ESI MS in combination with a continuous flow mixing technique. During ESI, intact gas phase ions are formed from protonated proteins in solution [for reviews, see Loo (1995), Przybylski and Glocker (1996), and Kebarle and Tang (1993)]. Different protein conformations can be detected by the different charge state distributions that they generate during ESI. In

† Supported by an NSERC-SCIEX Industrial Chair and the University of British Columbia. The rapid scanning stopped-flow spectrometer was purchased through MRC Major Equipment Grant ME-13015.

* Corresponding author. Phone: 604-822-3057. FAX: 604-822-2847. E-mail: douglas@chem.ubc.ca.

‡ Department of Chemistry.

§ Department of Biochemistry and Molecular Biology.

⊗ Abstract published in *Advance ACS Abstracts,* May 1, 1997.

[1] Abbreviations: aMb, apo-myoglobin (=myoglobin without heme group); aMb20, aMb21, etc., apo-myoglobin + 20 H^+, apo-myoglobin + 21 H^+, etc.; CAD, collisionally activated dissociation; CD, circular dichroism; ESI, electrospray ionization; ESI MS, electrospray ionization mass spectrometry; hMb, holo-myoglobin; hMb10, hMb11, etc., holo-myoglobin + 10 H^+, holo-myoglobin + 11 H^+, etc.; ID, inner diameter; *M*, protein mass; Mb, myoglobin; *m*/*z*, ratio of mass to charge for a given ion; RR, resonance Raman.

S0006-2960(97)00353-X CCC: $14.00

general, unfolded proteins exhibit higher charge states than proteins in a native-like conformation (Chowdhury et al., 1990; Loo et al., 1990; Katta & Chait, 1991; Mirza et al., 1993; Hamdan & Curcuruto, 1994; Przybylski & Glocker, 1996). Most early ESI MS experiments with hMb have been conducted under non-native conditions at low pH, where the protein exhibits high charge states and a mass corresponding to that of the apoprotein (Mann et al., 1989; Van Berkel et al., 1990; Cox et al., 1993; Covey & Douglas, 1993). However, later it was demonstrated that the intact heme−globin complex of hMb can also be detected by ESI MS, indicating that the noncovalent interactions between the heme and the protein can be preserved during ESI under appropriate conditions (Katta & Chait, 1991; Li et al., 1993; Jaquinod et al., 1993; Feng & Konishi, 1993; Konishi & Feng, 1994; Collings & Douglas, 1996; Hunter et al., 1997). The charge state distribution in the ESI mass spectrum of Mb strongly depends on the pH of the solution (Katta & Chait, 1991). At pH 3.35, only highly charged states of the apoprotein (M = 16 952 Da) are observed, indicating that under these conditions the contacts between the heme and the protein are disrupted and that the protein is in an unfolded state. At pH 4.4, the ESI mass spectrum shows only low charge states of the holoprotein (M = 17 568 Da) which is attributed to the fact that the protein has a more tighly folded conformation with heme−protein interactions that are sufficiently strong to prevent dissociation of the complex during ESI.

The kinetics of acid-induced hMb denaturation have been investigated previously by stopped-flow experiments (Shen & Hermans, 1972a,b,c). The measured exponential lifetimes showed a pronounced decrease with increasing acidity of the solution. It was suggested that unfolding of the protein precedes the destruction of the heme−protein interactions, although no direct evidence for this hypothesis could be given (Shen & Hermans, 1972c). Based on titration experiments, Hargrove et al. (1994a) and Hargrove and Olson (1996) proposed a scheme for hMb denaturation which seems to differ from that of Shen and Hermans. According to this second model, the protein first loses its heme to form a native-like structure of the apoprotein that later unfolds.

In this work, the kinetics of acid-induced hMb denaturation are monitored by time-resolved ESI MS to gain additional insight into the mechanism of the reaction. Time-resolved ESI MS offers the unique opportunity to monitor the folding state and the mass of the protein simultaneously as a function of time. The kinetics observed in these experiments are correlated with new results obtained from stopped-flow optical absorption spectroscopy that are also presented here. The data indicate that acid denaturation of hMb involves the formation of a partly unfolded transient hMb intermediate followed by disruption of the heme−protein interactions.

EXPERIMENTAL PROCEDURES

Chemicals. Horse heart Mb was obtained from Sigma (St. Louis, MO) and used without further purification. HPLC-grade glacial acetic acid was obtained from Fisher Scientific (Nepean, Canada).

Time-resolved ESI MS was carried out as described previously (Konermann et al., 1997). Briefly, two syringes (1 mL total volume each) were simultaneously advanced by a syringe pump. One syringe contained 40 μM Mb in water (pH 6.5), and the other contained a 0.45% solution (v/v) of acetic acid in water. The experiments were performed without using an internal standard. Initiation of Mb denaturation was triggered by mixing the liquids from both syringes in a tee, to produce a final pH of 3.2. The tee was connected to an ESI source by a "reaction capillary" with an inner diameter of 75 μm. The reaction time was controlled by the length of this reaction capillary. Capillary lengths varied between 0.9 and 186 cm corresponding to reaction times between 0.07 and 15.1 s, respectively. The total flow rate was kept constant throughout the experiment at 33 μL/min. Multiply charged gas phase proteins were generated by pneumatically assisted ESI and were analyzed by a quadrupole mass spectrometer constructed in house (Konermann et al., 1997). Depending on the voltage settings in the ion sampling interface, the heme−protein interactions in hMb can be disrupted by CAD in the interface region of the mass spectrometer (Collings & Douglas, 1996; Hunter et al., 1997). For this work, the voltage difference between the orifice and the RF-only quadrupole was +26 V. Under these conditions, no dissociation of the heme−protein complex was observed when electrosprayed under native conditions. A further decrease in this voltage difference was found to result in a pronounced "tailing" of the observed peaks on the high mass side that was probably caused by inefficient desolvation of the ions. Experiments were carried out at room temperature (21 ± 2 °C).

Stopped-flow experiments were carried out with an Olis-RSM 1000 rapid scanning stopped-flow absorption spectrometer (Bogart, GA), the observation cell of which had a 1 cm path length. Conditions for hMb denaturation were identical to those of the time-resolved ESI MS experiments with the exception that the final protein concentration after mixing was 5 μM. The temperature of the solutions was held constant at 21 °C.

Data Analysis. The time courses of intensity changes for the peaks in the mass spectrum, $I(m/z, t)$, and of the absorbance changes, $A(\lambda, t)$, respectively, were found to be well described by a sum of two exponentials plus a constant term:

$$I(m/z, t) = a_1(m/z)\exp(-t/T_1) + a_2(m/z)\exp(-t/T_2) + a_3(m/z) \quad (1)$$

$$A(\lambda, t) = a_1(\lambda)\exp(-t/T_1) + a_2(\lambda)\exp(-t/T_2) + a_3(\lambda) \quad (2)$$

In these equations, m/z is the mass to charge ratio for a given peak in the mass spectrum, t is the time after initiation of protein denaturation, λ is the wavelength, T_1 and T_2 are the exponential lifetimes with their corresponding amplitudes $a_1(m/z)$, $a_2(m/z)$, and $a_1(\lambda)$, $a_2(\lambda)$, respectively, and $a_3(m/z)$ and $a_3(\lambda)$ are the amplitudes of the nondecaying components. The kinetics of intensity changes for all peaks in the mass spectrum were analyzed simultaneously by the method of "global analysis" (Beechem et al., 1985). The same concept was applied to the absorption kinetics. The basis of global analysis is the assumption that changes throughout the whole spectrum exhibit the same lifetimes but differ in their amplitudes (Holzwarth, 1997). Error limits for the measured lifetimes were estimated as described previously (Konermann et al., 1997).

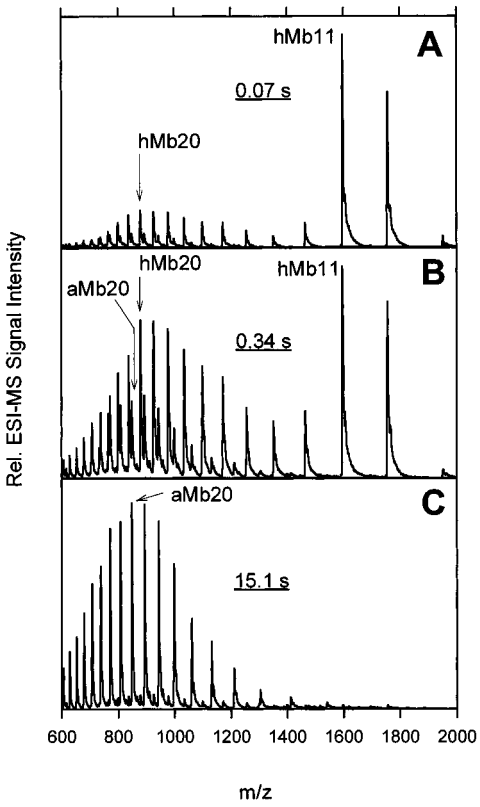

FIGURE 1: ESI mass spectra of Mb at different times after a pH-jump from 6.5 to 3.2; the spectra were recorded after 0.07 s (A), 0.34 s (B), and 15.1 s (C). Notation: hMb20 = holo-myoglobin + 20 H^+; aMb20 = apo-myoglobin + 20 H^+, etc.

RESULTS

ESI mass spectra of Mb recorded at different times after a pH-jump from 6.5 to 3.2 are shown in Figure 1. The spectrum obtained after 70 ms (Figure 1A) exhibits a bimodal distribution of hMb charge states with a primary maximum at hMb11 and a secondary maximum around hMb20. These two groups of peaks are attributed to populations of hMb having a native-like and a more unfolded conformation in solution, respectively. Closer inspection reveals the presence of some minor aMb peaks in the spectrum. After 0.34 s (Figure 1B), the relative contribution of hMb in high charge states is drastically increased and that of the low hMb charge states has decreased, indicating that more of the hMb has adopted the unfolded conformation in solution. Also, in Figure 1B the contribution of aMb peaks in the spectrum has increased over that of Figure 1A. The charge state distribution of the aMb peaks is centered at around aMb20 which indicates that the apoprotein is also in an unfolded conformation [aMb under native conditions at pH 6.5 produces a charge state distribution peaking at ~aMb10 (L. Konermann, to be published)]. The aMb peaks dominate the spectrum recorded after 15.1 s (Figure 1C); those of hMb have a total contribution of <5%. The spectrum depicted in Figure 1C is similar to the stationary spectrum of Mb recorded at pH 3.2, but the latter shows an even smaller contribution from hMb peaks (data not shown). Under the experimental conditions used in this study, the dissociated heme appears as a weak peak at $m/z = 615$ ($heme^{1+}$). The data shown in Figure 1 demonstrate that after a pH-jump from 6.5 to 3.2, the native protein is eventually transformed into an unfolded form with strongly diminished heme−protein interactions. During this process, a transient intermediate is formed which is considerably unfolded but still binds the heme with sufficient strength to prevent the dissociation of the complex during ESI.

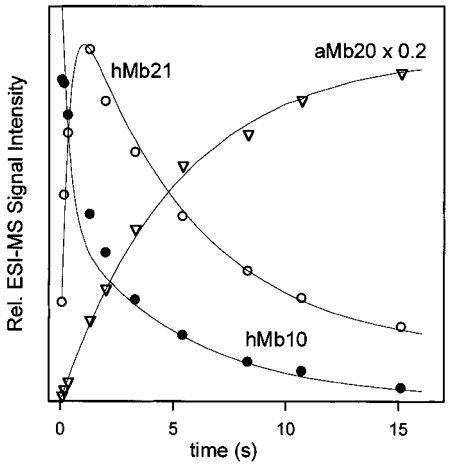

FIGURE 2: Time course of the signal intensity for three peaks in the ESI mass spectrum of Mb after a pH-jump from 6.5 to 3.2. The first data point in each curve represents $t = 0.07$ s. Solid lines are fits to the data by global analysis (see text). Note that the curve for aMb20 has been multiplied by a factor of 0.2. Data shown in this figure are the average of four sets of experiments. For explanation of abbreviations, see the caption to Figure 1.

To analyze the kinetics of this process further, the intensities of individual hMb and aMb peaks in the ESI mass spectrum were monitored as a function of time. Measurements were made from 70 ms to 15.1 s after the pH-jump. Typical data are shown in Figure 2 and represent the average of four sets of experiments. Solid lines are the result of a global fitting procedure (see below). Low charge states of the holo-protein, e.g., hMb10, decay rapidly. Concurrently, an increase in the intensity of more highly charged hMb peaks is observed on the same time scale, as exemplified by hMb21. The latter peaks reach maximum intensity after about 1 s and reflect the formation of unfolded hMb as a kinetic intermediate. Subsequently, these peaks decay considerably more slowly. This much slower process is accompanied by an increase of highly charged aMb peaks (for example, aMb20 in Figure 2). To describe the observed kinetics quantitatively, a global data analysis was carried out. For this fitting procedure, the exponential lifetimes T_i were the same for all the charge states in the spectrum, and only their amplitudes $a_i(m/z)$ differed [see Experimental Procedures and Konermann et al. (1997)]. The charge states hMb10 to hMb22 and aMb15 to aMb21 were included in the analysis. Higher charge states were not considered owing to increasing spectral overlap of the holo- and apo-protein peaks. The kinetics for all the charge states included in the analysis were found to be well fit by a sum of two exponentials and a constant term ($\chi^2 = 0.009$). As representative examples, the fits for three charge states are depicted in Figure 2 (solid lines). The two exponential lifetimes obtained from the analysis are $T_1 = 0.38 \pm 0.06$ s and $T_2 = 6.1 \pm 0.5$ s.

The amplitude spectra of these two lifetimes, sometimes referred to as "decay-associated spectra" (Beauregard et al., 1991), are shown in Figure 3 together with the amplitude spectrum of the nondecaying component. Positive amplitudes reflect a decay and negative amplitudes represent an increase in intensity with time. Therefore, eq 1 can describe

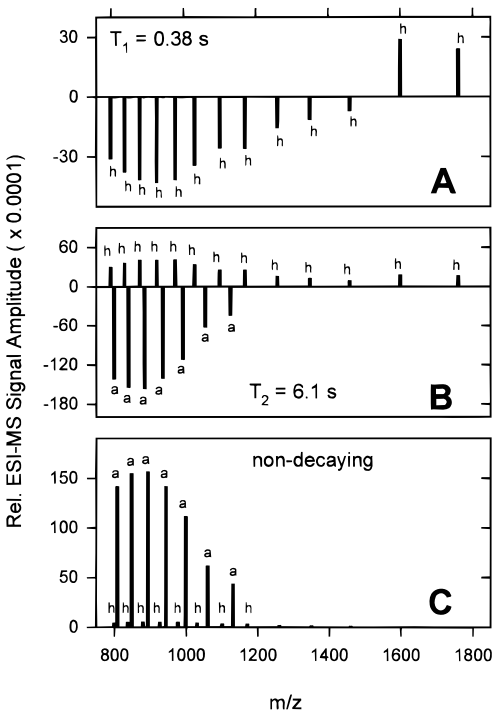

FIGURE 3: Amplitude spectra for the exponential lifetimes associated with the changes in the ESI mass spectrum of Mb after a pH-jump from 6.5 to 3.2: (A) for lifetime $T_1 = 0.38$ s, (B) for lifetime $T_2 = 6.1$ s, and (C) the nondecaying component. Data depicted in this figure have been obtained by global data analysis (see text). "h" and "a" denote charge states assigned to holo- and apomyoglobin, respectively.

both a rise and a fall of the intensities. The spectrum for the fast component T_1 exhibits positive amplitudes for hMb10 and hMb11 and negative amplitudes for all the higher charge states of hMb whereas the aMb peaks have an amplitude close to zero (Figure 3A). Therefore, this process reflects the transition from native-like hMb to the more unfolded state of hMb. The slower component T_2 has a completely different amplitude spectrum (Figure 3B). Here, the formation of unfolded aMb is reflected by the negative amplitudes for the respective charge states throughout the spectrum. The amplitude spectrum for hMb is entirely positive and has a maximum at around hMb19 that corresponds to the decay of unfolded hMb. The spectrum of the nondecaying component (Figure 3C) extrapolates the charge state distribution for infinite time after the pH-jump and is very similar to the spectrum shown in Figure 1C. It consists almost entirely of aMb charge states.

To characterize the acid-induced denaturation of Mb further, stopped-flow experiments were carried out using the same solution conditions as employed in the MS experiments. The change in the Soret region of the heme absorption spectrum as a function of time after a pH-jump from 6.5 to 3.2 is shown in Figure 4. The first spectrum recorded after the pH-jump ("$t = 0.0$ s") shows a relatively narrow absorption band with a maximum at around 409 nm. This maximum is red-shifted by ~1 nm relative to the absorption spectrum of Mb before the pH-jump whereas the maximum absorption coefficient of the protein remains constant (data not shown). A similar shift was previously observed for sperm whale Mb, and it was suggested that it is probably not caused by a major conformational change of the protein (Shen and Hermans, 1972a). During acid-induced denaturation of the protein, the Soret band decreases in intensity, and a product with a much broader, blue-shifted absorption spectrum is formed ($\lambda_{max} \sim 370$ nm). These spectral changes do not exhibit an isosbestic point, which indicates that the reaction cannot be described by a simple two-state mechanism. The kinetics for three selected wavelengths, 341, 409, and 441 nm, are depicted in Figure 5. The absorption at 409 nm undergoes a relatively slow decay that is accompanied by an increase on the blue side of the spectrum on the same time scale (as depicted for the curve measured at 341 nm). The absorption measured at 441 nm reveals the presence of a second, more rapid kinetic component that leads to an absorption increase at this wavelength. After ~2 s, this curve also shows a decrease in intensity and, therefore, reflects the formation of a kinetic intermediate. To correlate these data with those obtained by time-resolved ESI MS further, the kinetic data were subjected to global analysis. Again, the kinetics of the spectroscopic changes between 330 and 440 nm could be described well by the sum of two exponentials and a nondecaying component ($\chi^2 = 0.00016$). The exponential lifetimes were found to be T_1

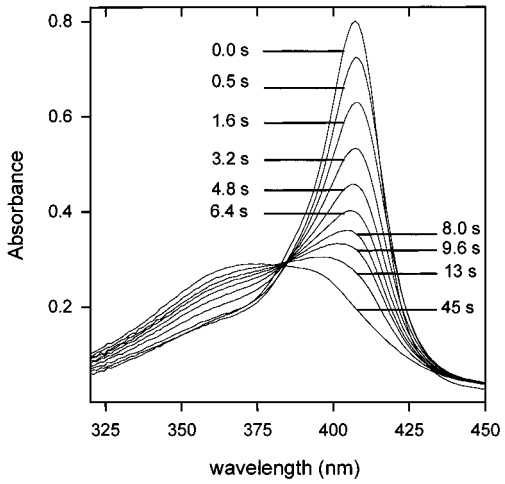

FIGURE 4: Absorption spectra of the Mb Soret region recorded at different times after a pH-jump from 6.5 to 3.2. The corresponding time for each spectrum is denoted in the figure.

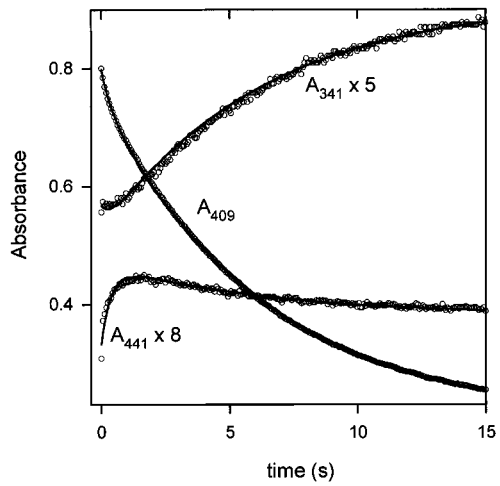

FIGURE 5: Changes in the Soret absorption of Mb measured at 341, 409, and 441 nm after a pH-jump from 6.5 to 3.2 vs time. Solid lines are fits to the experimental data (depicted as circles) and were obtained from global analysis (see text). Note that the curves recorded at 341 and 441 nm are multiplied by 5.0 and 8.0, respectively.

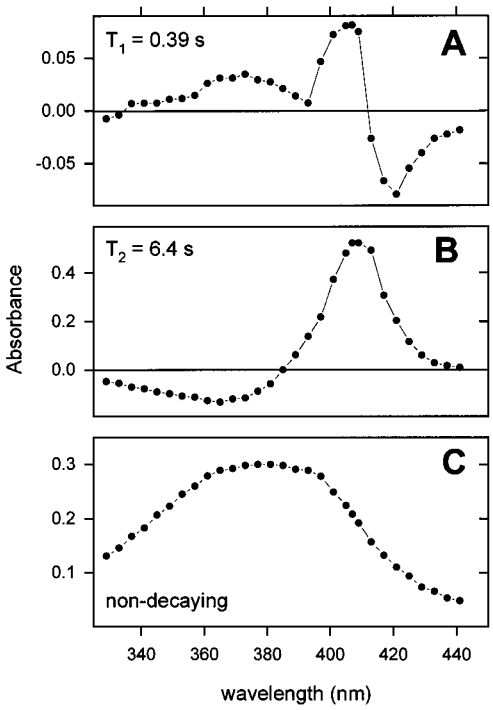

FIGURE 6: Amplitude spectra for the exponential lifetimes associated with the changes in the Soret absorption of Mb after a pH-jump from 6.5 to 3.2: (A) $T_1 = 0.39$ s, (B) $T_2 = 6.4$ s, and (C) nondecaying component. The fits depicted in this figure have been obtained by global data analysis (see text).

$= 0.39 \pm 0.03$ s and $T_2 = 6.4 \pm 0.4$ s. These values compare well with the lifetimes measured by time-resolved ESI MS ($T_1 = 0.38 \pm 0.06$ s and $T_2 = 6.1 \pm 0.5$ s, see above). For the kinetics monitored at 341, 409, and 441 nm, the fits are shown by the solid lines in Figure 5.

The amplitude spectra for the two kinetic components and for the nondecaying component are depicted in Figure 6. The amplitudes for the fast component ($T_1 = 0.39$ s) are positive from 340 to 409 nm and have a maximum at ~409 nm (Figure 6A). In this range, the kinetic processes lead to a decrease in absorption whereas from 412 to 440 nm the reverse is true as indicated by the negative amplitudes in that range. The processes on this time scale, therefore, lead to a shift of the absorption spectrum to the red. Indeed, close inspection of the spectra in Figure 4 reveals that the spectra recorded after 0.5 and 1.6 s, for example, extend slightly more to the red than observed for the first spectrum recorded after the pH-jump ("$t = 0.0$ s"). The second lifetime, $T_2 =$ 6.4 s, is associated with the major absorption changes that accompany the denaturation of Mb, namely, the successive decay of the Soret band at ~409 nm and the formation of a product with a broad, blue-shifted spectrum. This correlation is reflected by the positive amplitudes near 409 nm and the negative amplitudes near 370 nm (see Figure 6B). The spectrum of the nondecaying component depicted in Figure 6C represents the spectrum extrapolated to infinite time after the pH-jump and is similar to the spectrum recorded after 45 s (Figure 4). For this analysis, only the absorption changes occurring within 15 s after the pH-jump were included. If the analysis is extended to a total time range of 45 s, an additional time constant on the order of tens of seconds is found that exhibits very low amplitudes (lower than those for T_1). This additional component may reflect a small subpopulation of slowly unfolding proteins.

DISCUSSION

In this work, the pH-induced denaturation of hMb following a pH-jump from 6.5 to 3.2 was investigated by time-resolved ESI MS and stopped-flow absorption spectroscopy. The Soret region of the heme absorption is well-known to be an indicator of heme−protein interactions in Mb. Native hMb is characterized by a Soret maximum at ~409 nm. For acid-denatured Mb, the molar absorption coefficient is reduced by roughly 60%, and the Soret maximum is blue-shifted to ~370 nm (Shen & Hermans, 1972a; Puett, 1973; Bismuto et al., 1983; Sage et al., 1991; Palaniappan & Bocian, 1994; Hargrove et al. 1994b; Bogumil et al., 1995; Gupta et al., 1996). In the ESI mass spectrum, the acid-induced denaturation of the protein induces a shift from low charge states of hMb to high charge states of aMb (Katta & Chait, 1991). However, the complete disruption of the heme−protein interactions observed in these mass spectrometric experiments might not fully reflect the situation in solution. In the pH range used in this study, the heme most likely remains associated with the acid-denatured protein despite the loss of the iron−His^{93} linkage, thus forming a weak noncovalently associated complex (Sage et al., 1991). This complex is probably dissociated either during the ESI process itself or by CAD in the interface region of the mass spectrometer. Under harsher experimental conditions, this dissociation can also be achieved for native hMb (Collings & Douglas, 1996; Hunter et al., 1997). Control experiments confirmed that under the conditions used in the present study the dissociation of the native heme−globin complex was negligible (see Experimental Procedures).

The exponential lifetimes measured by time-resolved ESI MS and by stopped-flow absorption agree well. In both cases, the observed kinetics throughout the whole spectral range used for the analysis for times between 0 and 15 s could be well described by two lifetimes of about 0.4 and 6 s, respectively, plus a nondecaying component. The fast kinetic component was shown to be associated with the formation of a transient intermediate. The ESI mass spectrum of this intermediate shows charge states similar to those of acid-denatured Mb. However, these mass to charge ratios correspond to the mass of the intact heme−protein complex. Thus, the transient intermediate can be characterized as a form of hMb which is relatively unfolded compared to the native protein. The heme−protein interactions in this intermediate are not disrupted during ESI which indicates that the conformational changes at this stage do not lead to a substantial weakening of the heme binding. The absorption spectra (Figure 4) and the absolute values of the amplitudes of the short lifetime (Figure 6) clearly show that only relatively small changes in the heme absorption occur on the 0.4 s time scale. This observation implies that the environment of the heme in this intermediate resembles that of native hMb. From the data presented in Figures 4 and 6, it follows that the absorption spectrum of this folding intermediate is slightly shifted to the red and has its maximum absorption coefficient reduced by ~10% from that of native hMb. A more detailed structural characterization of this transient species should be possible by other techniques such as stopped-flow CD and/or continuous flow RR spectroscopy (Han et al., 1990).

The structural changes of the protein on the 6 s time scale lead eventually to the almost exclusive appearance of aMb

charge states in the ESI mass spectrum. This observation shows that these slower denaturation processes also affect the heme-binding pocket and lead to a substantial weakening of the heme−protein interactions. Simultaneously, the absorption spectrum undergoes a dramatic change which is probably associated with the breakage of the coordination bond between the heme iron and His^{93} (Sage et al., 1991). The data presented in this work thus clearly favor a sequential mechanism for the acid-induced denaturation of hMb that can be summarized in the following scheme:

$$(\text{heme}-\text{protein})_{\text{native}} \rightarrow (\text{heme}-\text{protein})_{\text{unfolded}} \rightarrow \text{heme} + (\text{protein})_{\text{unfolded}}$$

This mechanism was proposed initially by Shen and Hermans (1972a,b,c). On the basis of their stopped-flow absorption measurements, these authors suggested that during acid-induced denaturation the protein unfolds more rapidly than the heme−protein interactions are destroyed. However, on the basis of their data, alternative mechanisms could not be ruled out completely (Shen and Hermans, 1972c). The suggestions of Shen and Hermans seem to be in conflict with a model by Hargrove et al. (1994a) and Hargrove and Olson (1996), who proposed that the interactions between the heme and the protein are disrupted to form a native-like conformation of aMb that subsequently unfolds. This alternate mechanism was suggested on the basis of titration experiments under equilibrium conditions using guanidinium chloride and/or acid as denaturants [see references in Hargrove et al. (1994a)]. The data presented in this work for the acid-induced denaturation of hMb clearly support the mechanism proposed by Shen & Hermans. However, the mechanism suggested by Hargrove et al. may apply in case of other denaturants. In addition, the mechanisms observed under equilibrium and under nonequilibrium conditions might differ. Shen and Hermans (1972a) found considerably shorter lifetimes ($T_1 \approx 8$ ms and $T_2 \approx 140$ ms) for the denaturation of hMb under comparable pH conditions. These experiments were carried out by using a different type of Mb (sperm whale Mb in their study vs horse heart Mb here) and a citrate−KCl buffer with an ionic strength of 0.2. Virtually salt-free solutions were used in our study. Stopped-flow experiments carried out in our laboratory with sperm whale Mb in a buffer having the same composition as the one used by Shen and Hermans gave very similar lifetimes to the ones found in their study (data not shown). ESI MS experiments under these conditions are difficult due to the strong interference of salts with the ESI process (Przybylski & Glocker, 1996). These observations indicate that the rate constants for the acid-induced denaturation of hMb show a significant dependence on the ionic strength of the solvent and/or on the type of Mb used in the experiments. However, these different conditions do not seem to change the mechanism of the reaction, i.e., the formation of an unfolded form of the holoprotein prior to the disruption of the native heme−protein interactions. Interestingly, the mechanism of hMb denaturation in solution following a pH-jump seems to be similar to that of hMb ions in the gas phase. Based on measurements of the collision cross sections for Mb ions, Collings and Douglas (1996) concluded that unfolding of hMb ions precedes the disruption of the heme−protein interactions.

In a previous study, it was demonstrated that the kinetics of conformational changes of proteins can be monitored by time-resolved ESI MS (Konermann et al., 1997). Different protein conformations in solution were detected by the different charge state distributions that they generate during ESI. In the present study, it is shown that this method can be extended to cases in which the change in conformation is associated with a change in mass, e.g., when the protein loses a prosthetic group. This approach offers the unique opportunity to obtain information about the folding state of a protein and of its mass as a function of time. The contributions of two proteins with different masses can be separated unequivocally from each other even when their charge state distributions cover the same m/z range. This characteristic is a significant advantage in comparison with optical spectroscopy, where overlapping spectral bands usually complicate the analysis of experimental data. However, at the current state of development, optical experiments can provide data with higher signal to noise ratio and better time resolution compared to time-resolved ESI MS.

ACKNOWLEDGMENT

We thank Dr. Bruce A. Collings for his assistance with operation of the mass spectrometer.

REFERENCES

Beauregard, M., Martin, I., & Holzwarth, A. R. (1991) *Biochim. Biophys. Acta 1060*, 271−283.
Beechem, J. M., Ameloot, M., & Brand, L. (1985) *Anal. Instrum. 14*, 379−402.
Bismuto, E., Colonna, G., & Irace, G. (1983) *Biochemistry 22*, 4165−4170.
Bogumil, R., Maurus, R., Hildebrand, D. P., Brayer, G., & Mauk, A. G. (1995) *Biochemistry 34*, 10483−10490.
Chowdhury, S. K., Katta, V., & Chait, B. T. (1990) *J. Am. Chem. Soc. 112*, 9012-9013.
Collings, B. A., & Douglas, D. J. (1996) *J. Am. Chem. Soc. 118*, 4488−4489.
Covey, T., & Douglas, D. J. (1993) *J. Am. Soc. Mass Spectrom. 4*, 616−623.
Cox, K. A., Julian, R. K., Cooks, R. G., & Kaiser, R. E. (1994) *J. Am. Soc. Mass Spectrom. 5*, 127−136.
Evans, S. V., & Brayer, G. D. (1990) *J. Mol. Biol. 213*, 885−897.
Feng, R., & Konishi, Y. (1993) *J. Am. Soc. Mass Spectrom. 4*, 638−645.
Griko, Y. V., Privalov, P. L., Venyaminov, S. Y., & Kutshenko, V. P. (1988) *J. Mol. Biol. 202*, 127−138.
Gupta, R., Ydav, S., & Ahmad, F. (1996) *Biochemistry 35*, 11925−11930.
Hamdan, M., & Curcuruto, O. (1994) *Rapid. Commun. Mass Spectrom. 8*, 144−148.
Han, S., Rousseau, D. L., Giacometti, G., & Brunori, M. (1990) *Proc. Natl. Acad. Sci. U.S.A. 87*, 205−209.
Hargrove, M. S., & Olson, J. S. (1996) *Biochemistry 35*, 11310−11318.
Hargrove, M. S., Krzywda, S., Wilkinson, A., Dou, Y., Ikeda-Saito, M., & Olson, J. S. (1994a) *Biochemistry 33*, 11767−11775.
Hargrove, M. S., Singleton, E. W., Quillin, M. L., Ortiz, L. A., Phillips, G. N., & Olson, J. S. (1994b) *J. Biol. Chem. 269*, 4207−4214.
Hargrove, M. S., Barrick, D., & Olson, J. S. (1996a) *Biochemistry 35*, 11293−11299.
Hargrove, M. S., Wilkinson, A. J., & Olson, J. S. (1996b) *Biochemistry 35*, 11300-11309.
Holzwarth, A. R. (1997) in *Biophysical Techniques* (Amesz, J., & Hoff, A., Eds.) Kluwer Academic Publishers, Dordrecht, Holland (in press).
Hughson, F. M., Wright, P. E., & Baldwin, R. L. (1990) *Science 249*, 1544−1548.

Hunter, C. H., Mauk, A. G., & Douglas, D. J. (1997) *Biochemistry 36*, 1010−1025.
Jaquinod, M., Leize, E., Potier, J., Albrecht, A.-M., Shauzer, A., & Dorsselaer, A. (1993) *Tetrahedron Lett. 34*, 2771−2774.
Katta, V., & Chait, B. T. (1991) *J. Am. Chem. Soc. 113*, 8534−8535.
Kebarle, P., & Tang, L. (1993) *Anal. Chem. 65*, 972−986.
Konermann, L., Collings, B. A., & Douglas, D. J. (1997) *Biochemistry* (submitted for publication).
Konishi, Y., & Feng, R. (1994) *Biochemistry 33*, 9706−9711.
Li, Y. T., Hsieh, Y. L., Henion, J. D., & Ganem, B. (1993) *J. Am. Soc. Mass Spectrom. 4*, 631−637.
Loo, J. A. (1995) *Bioconjugate Chem. 6*, 644−665.
Loo, J. A., Edmonds, C. G., Udseh, H. R., & Smith, R. D. (1990) *Anal. Chem. 62*, 693−698.
Mann, M., Meng, C. K., & Fenn, J. B. (1989) *Anal. Chem. 61*, 1702−1708.
Mirza, U. A., Cohen, S. L., & Chait, B. T. (1993) *Anal. Chem. 65*, 1−6.
Palaniappan, V., & Bocian, D. F. (1994) *Biochemistry 33*, 14264−14274.
Prybylski, M., & Glocker, M. O. (1996) *Angew. Chem., Int. Ed. Engl. 35*, 806−826.
Puett, D. (1973) *J. Biol. Chem. 248*, 4623−4634.
Rossi-Fanelli, A., Antonini, E., & Caputo, A. (1958) *Biochim. Biophys. Acta 30*, 608−615.
Sage, J. T., Morikis, D., & Champion, P. M. (1991) *Biochemistry 30*, 1227−1237.
Shen, L. L., & Hermans, J. (1972a) *Biochemistry 11*, 1836−1841.
Shen, L. L., & Hermans, J. (1972b) *Biochemistry 11*, 1842−1844.
Shen, L. L., & Hermans, J. (1972c) *Biochemistry 11*, 1845−1849.
Takano, T. (1977) *J. Mol. Biol. 110*, 537−568.
Teale, F. W. (1959) *Biochim. Biophys. Acta 35*, 543.
Van Berkel, G. J., Glish, G. L., & McLuckey, S. A. (1990) *Anal. Chem. 62*, 1284−1295.

BI970353J